Revisiting M-shell binding energies for elements with $72 \leqslant Z \leqslant 83$

Jorge Trincavelli,[1] Gustavo Castellano,[1] Silvina Segui,[1] Silvina Limandri,[1] María del Rosario Torres Deluigi,[2] Claudia Montanari,[3] Darío Mitnik,[3] and Alejo Carreras[1,*]

[1]*Instituto de Física Enrique Gaviola (IFEG-CONICET), Facultad de Matemática, Astronomía, Física y Computación (FAMAF), Universidad Nacional de Córdoba, Córdoba, Argentina*

[2]*Instituto de Química de San Luis (INQUISAL-CONICET) – Universidad Nacional de San Luis, San Luis, Argentina*

[3]*Instituto de Astronomía y Física del Espacio (IAFE-CONICET) – Universidad de Buenos Aires, Buenos Aires, Argentina*

(Received 27 October 2023; accepted 15 March 2024; published xxxxxxxxxx)

Experimental M_4 and M_5 cross-section curves of some sixth-period elements were observed to exhibit an abnormal crossover above 20 keV, when the M_5 binding energy is taken from the most commonly used databases available in the literature for the assessment of absorption effects [Aguilar, Castellano, Segui, Trincavelli, and Carreras, J. Anal. At. Spectrom. **38**, 751 (2023)]. This clearly suggests the need for a revision of the published binding-energy values [Bearden and Burr, Rev. Mod. Phys. **39**, 125 (1967); Larkins, At. Data Nucl. Data Tables **20**, 311 (1977)]. The self-absorption effects of the $M\beta$ line and of bremsstrahlung in an energy region close to the M_5 binding energy were analyzed by using energy and wavelength dispersive spectroscopy, respectively. An important inconsistency in the x-ray absorption was found when assessed accordingly with the literature, which led to shift the M_5-edge positions of Re, Os, Ir, and Pt. In the particular case of rhenium, theoretical calculations have been performed to assess M binding energies. To this end, the many-electron Dirac equation was numerically solved to estimate the configuration energies associated with M_5 one-vacancy states. The binding energies obtained are consistent with the present experimental results, and with the most widely accepted characteristic-energy values.

DOI: 10.1103/PhysRevA.00.002800

I. INTRODUCTION

X-ray attenuation in matter is involved in many areas ranging from radiation therapies to materials characterization by means of spectroscopical techniques. To properly describe this attenuation, the knowledge of absorption edge positions, closely related to the binding energies of the electrons in the different atomic levels, is of crucial importance. The accuracy of these parameters directly impacts not only the many applications aforementioned but also a number of experiments related to the interaction of radiation with matter [1–6].

Despite the evident intrinsic importance of these binding energies as fundamental parameters in atomic physics, the data available in the literature, usually taken as reference values, have been measured more than four decades ago [7]. Unfortunately, little effort has lately been devoted to the experimental determination of these edges, although many technological advances have given rise to a number of new measurement tools.

To date, three experimental methods have been used to address the determination of binding energies. These methods are based on x-ray absorption spectroscopy (XAS), x-ray photoelectron spectroscopy (XPS), and x-ray emission spectroscopy techniques.

X-ray absorption spectroscopy is an approach used by several authors [8–12] and is based on the measurement of the fraction of x-ray photons transmitted through a thin sample as a function of the photon energy in an energy region close to the absorption edge. There are several criteria for determining the position of this edge, among which the location of the maximum of the derivative of the attenuation coefficient μ with respect to the incident energy is commonly chosen [13]. Thus, the uncertainties arising from these measurements involve errors associated with the experimental setup and also with the method used to determine the edge position in the spectrum.

In x-ray photoelectron spectroscopy, the inner-shell electrons are excited by incident photons of well-defined energy $h\nu$, and they are ejected with a kinetic energy E_K —measured by a spectrometer—, which in the frozen orbital approximation is related to the electron binding energy according to

$$E_K = h\nu - E_{\text{bin}} - \phi,$$

where E_{bin} is the photoelectron binding energy and ϕ is the spectrometer work function [14]. The photoelectron spectrum as a function of E_{bin} exhibits structures corresponding to the energies of the orbitals from which the photoelectrons are removed. The absorption edge is chosen as the position of the maximum of the structure associated with this edge. Nevertheless, it must be taken into account that when a photoelectron is removed, the ionized atom relaxes. Thus, some of the remaining electron orbitals decrease their energy imparting extra kinetic energy to the emitted electron. Therefore the measured binding energy should be lower than expected [15].

When x-ray emission spectroscopy is chosen, absorption edges are calculated as differences between characteristic

*alejocarreras@unc.edu.ar

energies, taking at least one absorption edge as reference. Bearden and Burr [7] used this approach by determining characteristic x-ray energies and combining them with a few absorption edges measured by XPS. It must be emphasized that the Bearden and Burr database is one of the most widely used today and these data are included in many recent compilations. According to this database, for elements with atomic number Z between 72 and 78, the M_5 binding energy E_{M_5} is slightly below the energy of the $M\beta$ emission line (M_4N_6 decay) [7,16–18], which implies a strong self-absorption of these characteristic x-rays when traversing the sample towards the detector.

The $M\beta$-line self-absorption in some sixth period elements depends critically on the E_{M_5} value, as well as on the mass absorption coefficient μ. In a recent study [19], an abnormal crossover between M_4 and M_5 cross sections was observed around 25 keV, when the M_5 binding energy is taken from the most commonly used databases available in the literature. This suggests the need of carefully studying the location of the M_5 absorption edge with respect to the $M\beta$ emission energy, since characteristic energies are known with higher precision.

The present work combines experimental and theoretical approaches to study the position of the M_5 absorption edge of some sixth-period elements. To this purpose, the bremsstrahlung absorption around the Re M_5 edge was surveyed by means of wavelength dispersive x-ray spectroscopy. In addition, for elements with atomic number Z between 72 and 83, the $M\alpha/M\beta$ ($M_5N_{6,7}/M_4N_6$) intensity ratios were determined by energy dispersive x-ray spectroscopy and compared with the corresponding predictions involving tabulated data for E_{M_5} and μ. Finally, fully relativistic calculations implemented by using the Hebrew University Lawrence Livermore Atomic Code (HULLAC) suite [20] were performed for solving the many-electron Dirac equation, to provide an estimate for the configuration energies associated with M_5 one-vacancy states.

II. EXPERIMENT

X-ray emission spectra for elements with $72 \leqslant Z \leqslant 83$ were obtained from pure bulk standards (Micro-Analysis Consultants, Ltd.). Since these polished standards are embedded in a nonconductive resin within a brass block, a carbon coating was used to ensure adequate conductivity. The thickness of the carbon layer was determined in a previous work [19] by measuring spectra from a region of the brass block close to the standards used. A thickness of (22.1 ± 0.8) nm was obtained from the spectral fit performed by means of the software POEMA [21]. Note that this carbon layer is thin enough and does not affect the assessments performed along this work.

The targets were irradiated with 5 and 20 keV electrons in a Carl Zeiss Σigma field emission scanning microscope. The x-ray spectra were acquired with an energy dispersive spectrometer (EDS), equipped with an Oxford silicon drift detector, whose front window is an ultrathin polymer layer, supported by a silicon grid 380 μm thick with 77% open area.

To study in detail one of the elements considered, several pure rhenium spectra were measured with an INCA WAVE 700 wavelength dispersive spectrometer (WDS) attached to a LEO 1450 VP scanning electron microscope, with an electron beam of 20 keV and 260–280 nA and a take-off angle of 29°. The arrangement of the WDS is Johansson type for the PET crystal used. A single spectrum was built by adding the spectra collected in order to achieve better statistics.

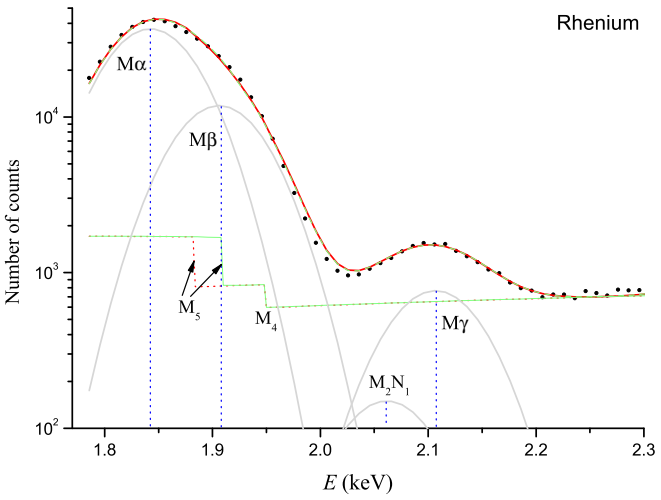

FIG. 1. Rhenium EDS spectrum for a 20 keV electron beam. Dots: experimental; red solid and green dashed lines: overall fits choosing different values for E_{M_5} edge; gray lines: diagram transitions; red thin dotted line: background choosing $E_{M_5} = 1883$ eV; green dotted line: background choosing $E_{M_5} = 1907$ eV.

III. SPECTRAL PROCESSING

All the spectra analyzed here were fitted by using a spectral processing tool previously developed and implemented in the software POEMA [21]. The spectral processing method consists in fitting a function to the experimental data by optimizing the instrumental and atomic parameters involved in the analytical description. The estimate provided for the x-ray intensity at the energy E is given by

$$N = B(E) + \sum_q P_q S_q(E), \tag{1}$$

where B is the background radiation, S_q is a function accounting for the peak shape, which, in the case of an EDS spectrum, is a Gaussian function corrected by peak asymmetry, and P_q is the intensity of the characteristic q line. For N_e incident electrons of energy E_i, this intensity is given by

$$P_{q,i} = N_e \tilde{\sigma}_{q,i} \omega_q p_q (\mathcal{Z}\mathcal{A}\mathcal{F})_{q,i} \varepsilon(E_q), \tag{2}$$

where $\tilde{\sigma}_{q,i}$ is the final vacancy production cross section of the atomic shell related to the q line evaluated at the energy E_i, ω_q is the corresponding fluorescence yield, p_q and E_q are the relative transition probability and the characteristic energy of the q line, respectively; $\mathcal{Z}$, $\mathcal{A}$, and $\mathcal{F}$ are related to the so-called atomic number, absorption and fluorescence correction factors, respectively, and ε is the spectrometer efficiency.

IV. RESULTS AND DISCUSSION

Figure 1 shows an EDS spectrum for rhenium induced by 20 keV electrons, along with two fitting curves relying on the mass absorption coefficients given in Ref. [22] for two

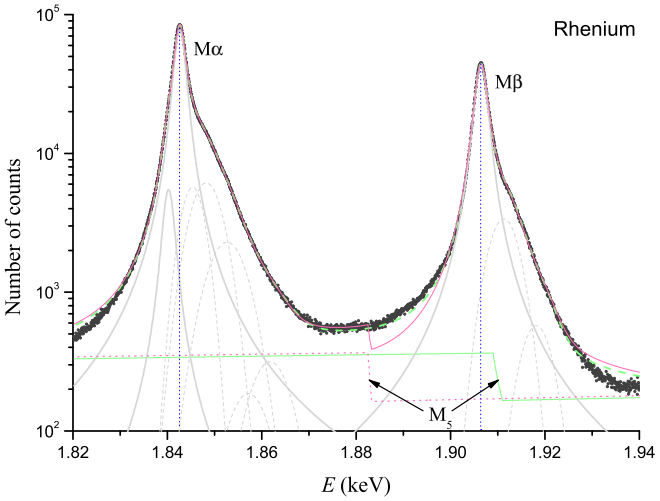

FIG. 2. Rhenium WDS spectrum. Dots: experimental; pink lines: fit (solid) and background (dotted) choosing $E_{M_5} = 1883$ eV; green lines: fit (dashed) and background (solid) choosing $E_{M_5} = 1907$ eV; gray solid lines: diagram transitions; gray dashed lines: satellite transitions.

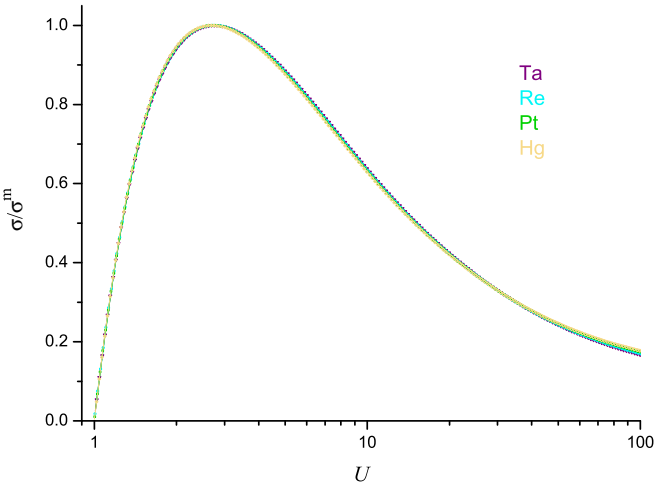

FIG. 3. Theoretical M_4 (lines) and M_5 (symbols) ionization cross sections σ based on the distorted wave Born approximation approach [27] for several elements, normalized to their corresponding maxima $\sigma^{\rm m}$, as a function of the overvoltage U.

different choices of E_{M_5}: 1883 eV, as given in Refs. [7,17], and a value of 1907 eV proposed here, as obtained by the theoretical calculations described below, slightly above the Re $M\beta$ emission energy. Although the final fits look quite similar, certain parameters involved in the spectral description bear very different values. When using the proposed E_{M_5} value, the absorption correction for the $M\beta$ line changes by a factor $\approx$2, strongly influencing the estimation of atomic parameters obtained from the spectral fitting, such as the M_4-subshell ionization cross section [19].

A WDS spectrum corresponding to the Re $M\alpha$–$M\beta$ region is shown in Fig. 2, which also displays the contribution of diagram and satellite lines in gray. Clearly, the predicted background contribution is not suitable when using the E_{M_5} value reported in Refs. [7,17], since the expected jump cannot be observed at 1883 eV in the experimental spectrum. A better spectral fitting is attained when the M_5 edge is shifted above the $M\beta$ emission energy. Notice that a jump in the background around 1907 eV would be concealed within the statistical fluctuations of the $M\beta$ peak.

Another approach that can help to survey the location of the M_5 absorption edge arises from comparing experimental and calculated $M\alpha/M\beta$ intensity ratios obtained with electrons impinging with two different beam energies, E_1 and E_0. By normalizing the $M\alpha/M\beta$ intensity ratio obtained with E_1 to that corresponding to a lower incident energy E_0, the influence of several relaxation and detection parameters (fluorescence yields, radiative transition probabilities, and spectrometer efficiency) can be readily avoided. In the present work, values of 20 and 5 keV were chosen for E_1 and E_0, respectively, which lead to clearly different absorption effects. Thus, theoretical $Q^{\rm theor}$ and experimental $Q^{\rm expt}$ ratios are defined as

$$Q^{\rm theor} = \frac{P_{\alpha,1}/P_{\beta,1}}{P_{\alpha,0}/P_{\beta,0}}, \tag{3}$$

and

$$Q^{\rm expt} = \frac{I_{\alpha,1}/I_{\beta,1}}{I_{\alpha,0}/I_{\beta,0}}, \tag{4}$$

where $I_{\alpha,i}$ and $I_{\beta,i}$ are the experimental intensities for $M\alpha$ and $M\beta$ emission lines at the incidence energy E_i, respectively. Equation (2) may be replaced in Eq. (3), obtaining

$$Q^{\rm theor} = \frac{\left[\tilde{\sigma}_{\alpha,1}(\mathcal{Z}\mathcal{A}\mathcal{F})_{\alpha,1}\right]/\left[\tilde{\sigma}_{\beta,1}(\mathcal{Z}\mathcal{A}\mathcal{F})_{\beta,1}\right]}{\left[\tilde{\sigma}_{\alpha,0}(\mathcal{Z}\mathcal{A}\mathcal{F})_{\alpha,0}\right]/\left[\tilde{\sigma}_{\beta,0}(\mathcal{Z}\mathcal{A}\mathcal{F})_{\beta,0}\right]}. \tag{5}$$

In this expression, it is expected that $\mathcal{Z}_{\alpha,i} \simeq \mathcal{Z}_{\beta,i}$ and $\mathcal{F}_{\alpha,i} \simeq \mathcal{F}_{\beta,i}$. On the one hand, the $\mathcal{Z}$ correction depends only on the overvoltage $U = E_i/E_{M_q}$ for a given element and $U_{\alpha,i} \simeq U_{\beta,i}$ for the incidence energies considered. Besides, the $\mathcal{F}$ correction is usually unimportant, particularly for the case of M lines, for which the fluorescence yield coefficients are very small. In fact, after numerical evaluation [21,23], it was observed that the ratio

$$\mathbb{ZF} = \frac{(\mathcal{Z}\mathcal{F})_{\alpha,1}/(\mathcal{Z}\mathcal{F})_{\beta,1}}{(\mathcal{Z}\mathcal{F})_{\alpha,0}/(\mathcal{Z}\mathcal{F})_{\beta,0}} \tag{6}$$

differs from unity by less than 3%. Therefore, Eq. (5) can be reduced to

$$Q^{\rm theor} \simeq \frac{[\tilde{\sigma}_{\alpha,1}\mathcal{A}_{\alpha,1}]/[\tilde{\sigma}_{\beta,1}\mathcal{A}_{\beta,1}]}{[\tilde{\sigma}_{\alpha,0}\mathcal{A}_{\alpha,0}]/[\tilde{\sigma}_{\beta,0}\mathcal{A}_{\beta,0}]}. \tag{7}$$

Several authors have described the ionization cross section using relatively simple expressions that depend mainly on the overvoltage and a few parameters related to the considered shell [24,25]. Furthermore, according to Ref. [26] a single function $f(U)$ depending on the overvoltage is a reasonable approach for cross-section curves, normalized to their corresponding maxima $\tilde{\sigma}_q^{\rm m}$ for different elements and shells. Particularly, this can be verified for M_4 and M_5 subshells in Fig. 3, which displays a set of ionization cross sections assessed by means of a sophisticated model [27] for several elements in the range of interest. The $\tilde{\sigma}$ ratios for beam energy

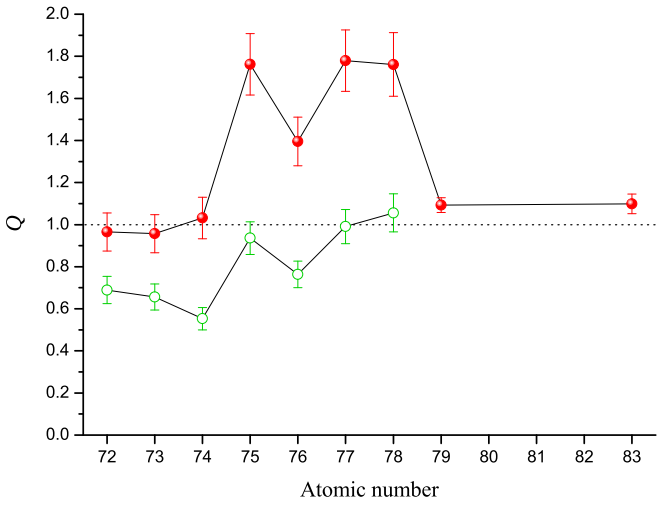

FIG. 4. Values obtained for the Q ratios as a function of the atomic number, using the E_{M_5} values from Refs. [7,17] (spheres), and modified values with E_{M_5} above the energy of the $M\beta$ line (open circles).

E_i can then be approximated as

$$\frac{\tilde{\sigma}_{\alpha,i}}{\tilde{\sigma}_{\beta,i}} = \frac{\tilde{\sigma}^{\mathrm{m}}_{\alpha} f(U_{\alpha,i})}{\tilde{\sigma}^{\mathrm{m}}_{\beta} f(U_{\beta,i})},$$

and thus the quotient

$$\mathbb{S} = \frac{\tilde{\sigma}_{\alpha,1}/\tilde{\sigma}_{\beta,1}}{\tilde{\sigma}_{\alpha,0}/\tilde{\sigma}_{\beta,0}} \tag{8}$$

is quite close to unity for all the elements considered in this work, because the maxima are canceled out and $U_{\alpha,i} \simeq U_{\beta,i}$ for both energies. Indeed, this ratio also differs from unity by less than 3%, as confirmed by a numerical assessment. Finally, Eq. (7) can be approximated by

$$Q^{\mathrm{theor}} \simeq \mathbb{A} = \frac{\mathcal{A}_{\alpha,1}/\mathcal{A}_{\beta,1}}{\mathcal{A}_{\alpha,0}/\mathcal{A}_{\beta,0}}, \tag{9}$$

To survey how accurate the theoretical approach provided by Q^{theor} may be, the parameter

$$Q = \frac{Q^{\mathrm{expt}}}{Q^{\mathrm{theor}}} \tag{10}$$

was assessed. If Q^{theor} is adequate, the factor Q must be close to unity. In Fig. 4, the factors Q obtained by using the E_{M_5} values from Refs. [7,17] and values arbitrarily shifted to lie slightly above the $M\beta$ energy are plotted as a function of Z for elements with $72 \leqslant Z \leqslant 83$. The evident deviation of Q from unity for Re, Os, Ir, and Pt, when using the E_{M_5} value from Refs. [7,17], suggests an inadequate assessment of Q^{theor} in Eq. (9), since the uncertainty in the determination of Q^{expt} in Eq. (4) is very low and similar for all the studied elements.

It is therefore clear that the deviation mentioned must be attributed to a problem in the assessment of the absorption correction. Particularly, the absorption of the $M\alpha$ line is almost independent of the M_5-edge position; instead, the estimation for the $M\beta$ line self-absorption is very sensitive to the value chosen for E_{M_5}, since if $E_{M_5} < E_{\mathrm{M}\beta}$, there is a strong self-absorption, whereas if $E_{M_5} > E_{\mathrm{M}\beta}$, the $M\beta$ line absorption effect is similar to that undergone by the $M\alpha$ line, because none of these characteristic decays can excite the M_5 level.

Therefore, the higher Q-ratio values for $75 \leqslant Z \leqslant 78$ displayed in Fig. 4 can be attributed to an incorrect location of the M_5 edge respect to the $M\beta$ line, which leads to a wrong evaluation of the self-absorption. Shifting E_{M_5} above the $M\beta$ emission energy yields better values for Q ratios in this Z range, although for lower Z values the M_5 binding energies published in Refs. [7,17] appear to be correct.

The estimation of the uncertainties displayed in Fig. 4 arises from error propagation in Eq. (10). Taking into account Eqs. (5), (6), (8), and (9), the uncertainty ΔQ can be expressed in terms of the uncertainties ΔQ^{expt}, $\Delta\mathbb{A}$, $\Delta(\mathbb{ZF})$, and $\Delta\mathbb{S}$ as

$$\left(\frac{\Delta Q}{Q}\right)^2 = \left(\frac{\Delta Q^{\mathrm{expt}}}{Q^{\mathrm{expt}}}\right)^2 + \left(\frac{\Delta\mathbb{A}}{\mathbb{A}}\right)^2 + \left(\frac{\Delta(\mathbb{ZF})}{\mathbb{ZF}}\right)^2 + \left(\frac{\Delta\mathbb{S}}{\mathbb{S}}\right)^2. \tag{11}$$

The first term corresponds to the propagation of statistical uncertainties in the intensities of Eq. (4), the second term is obtained by assessing the variation of the $\mathbb{A}$ factor arising from modifying the attenuation coefficient in 30%, according to Chantler [22], and the last two terms were evaluated as the departure of $\mathbb{ZF}$ and $\mathbb{S}$ from unity.

In a previous determination of x-ray production cross sections σ^{X} of Re ($Z = 75$) and Os ($Z = 76$) [19], a deviation of the M_4 subshell curve from the general trend was observed between 20 and 30 keV when using the E_{M_5} value reported in Refs. [7,17]. Particularly, a crossover of σ^{X} curves corresponding to M_4 and M_5 subshells occurs for osmium in this energy region, which contradicts the existence of a unique function that describes the behavior of the cross section in terms of the overvoltage [26]. It is worth mentioning that this crossover is observed to disappear when the edge energy is shifted above the $M\beta$ line.

The results obtained for the parameter Q, plotted in Fig. 4, show that the M_5 edge must be on the high-energy side of the $M\beta$ line for $Z \geqslant 75$, and very close to this line, as suggested by the fits displayed for rhenium in Fig. 2. For this reason, the experimental determination of the M_5 edge energy is not possible by this means, due to the strong overlapping observed with the $M\beta$ line, even with WDS resolution.

To study the location of the M_5 edge, the integrated code HULLAC [20,28] was used to assess the rhenium configuration energies for one-vacancy states in the $3d_{5/2}$ subshell (M_5), relative to the ground state. Through this software, the Dirac equation was numerically solved, including the Breit interaction energies and quantum electrodynamic corrections in first-order perturbation theory. The detailed level energies were calculated using the fully relativistic multiconfigurational RELAC code [29], based on the parametric potential model. The main idea of this model is to describe in a simple fashion the screening of some sensible parametrized charge distribution. This is done by the introduction of a central potential as an analytic function of the screening parameters, which are determined by minimizing the first-order relativistic energy of a set of configurations. This optimized potential is used to calculate all one-electron orbitals and energies,

relativistic multiconfiguration bound states and their energies, continuum orbitals, and all the required transition rates. The HULLAC code has been used in many atomic structure calculation of heavy elements, obtaining results in excellent agreement with the experimental ones (see, for example, Refs. [30–32]). In the present calculations, the potential was first optimized to minimize the energy of the Re ground state $[\mathrm{Xe}]4f^{14}5d^{5}6s^{2}$ mixed with the $[\mathrm{Xe}]4f^{14}5d^{6}6s$ configuration. Then, the $3d$ ionized Re^{+} (W-like) configuration $3d^{9}4f^{14}5d^{5}6s^{2}$ (mixed with $3d^{9}4f^{14}5d^{6}6s$) was optimized. This potential was used for further structure calculation, but the energies of the Re configurations were shifted to obtain the values they had with their own optimized potential. The theoretical spectrum of the $3d^{9}4f^{14}5d^{5}6s^{2}$ configuration shows two groups (separated by about 70 eV). The lower one has the hole in the $3d_{5/2}$ electron (M_5 transition), and the other group is formed by a $3d_{3/2}$-electron vacancy (M_4 transition). The effect of the configuration interaction in the Re ground level energies was studied by adding more configurations in the structure calculation—even trying double-excited configurations such as the $4f^{14}5d^{7}$—but no important contribution was found. Since this configuration is separated by more than 50 eV from the ground $4f^{14}5d^{5}6s^{2}$ configuration, the mixing is very small and does not affect the ionization energies.

To obtain a value of the M_5 edge comparable to data compiled in the literature, which were determined by means of photon incidence, the AUTOSTRUCTURE package [33–35] was used to assess photoionization cross sections. When considering inner-shell orbitals, relativistic effects must be taken into account. Although the AUTOSTRUCTURE code is not fully relativistic, it allows performing the calculations in a perturbative-relativistic intermediate-coupling mode based on a Breit-Pauli Hamiltonian. The code generates the semirelativistic bound orbital functions, following the approach proposed by Cowan and Griffin [36] in which the mass velocity and Darwin terms of the Pauli equation for one-electron atoms have been added to the usual nonrelativistic one-electron Hartree-Fock differential equations. Perturbation theory is used to evaluate the remaining one-body (namely, spin-orbit) and two-body fine-structure interactions (spin-other-orbit and spin-spin) and two-body non-fine-structure interactions (i.e., contact spin-spin, two-body Darwin and orbit-orbit operators). The continuum orbitals are calculated under the distorted-wave approximation. The spectra obtained with AUTOSTRUCTURE calculation has the same overall features than those obtained with HULLAC, i.e., two clearly separated energy-level groups were obtained, which are easily assigned to a hole in the $3d_{5/2}$ and in the $3d_{3/2}$ subshells. According to the present HULLAC results, the lowest level of the Re^{+} configuration that has an electron vacancy in the $3d_{5/2}$ subshell is $3d_{-}^{4}3d_{+}^{5}5d_{-}^{3}5d_{+}^{2}6s^{2}$, $J=5$. All the AUTOSTRUCTURE energy values for the levels belonging to this group were shifted an amount assessed as the difference of this lowest energy value calculated with HULLAC and AUTOSTRUCTURE. The difference obtained using both codes for the lowest level of the configuration with a hole in $3d_{3/2}$ ($3d_{-}^{3}3d_{+}^{6}5d_{-}^{3}5d_{+}^{2}6s^{2}$, $J=1$) is very similar to the previous one, and this value has been used in the AUTOSTRUCTURE calculations to displace all levels belonging to this second group.

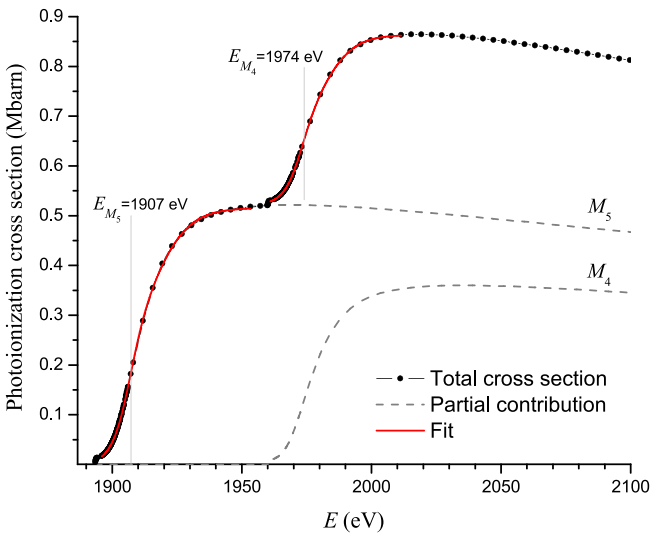

FIG. 5. Rhenium photoionization cross section calculated with the AUTOSTRUCTURE code. The positions of the M_5 and M_4 edges obtained are also displayed.

Summarizing, photoionization cross sections were calculated with AUTOSTRUCTURE, and the energies were shifted so that the $3d$ inner-shell ionized configuration energies coincided with the values determined by means of HULLAC, which is more reliable since this code involves a fully relativistic model. The total cross section curve was obtained as the sum of the contributions of the different levels; the positions of the M_5 and M_4 edges at (1907 ± 8) and (1974 ± 8) eV, respectively, were determined as the inflection points of this curve, as shown in Fig. 5. The uncertainties were estimated through the first derivative of the fitting function, and considering its width at half maximum.

It is interesting to note that the difference between these two values is consistent with the characteristic energies given by Bearden [16]. For instance, as the energies of the $L\alpha_1$ and $L\alpha_2$ lines satisfy

$$E_{L\alpha_1} = E_{L_3} - E_{M_5},$$

and

$$E_{L\alpha_2} = E_{L_3} - E_{M_4},$$

it follows

$$E_{L\alpha_1} - E_{L\alpha_2} = E_{M_4} - E_{M_5}. \tag{12}$$

According to Ref. [16], the first member of Eq. (12) is equal to 66.3 eV, and the value obtained here for the second member is 66.4 eV, showing an excellent agreement.

Table I displays the E_{M_5} values available for elements with atomic number between 70 and 83 (columns 3–9). The data published in Refs. [8–12] were obtained by absorption spectroscopy, whereas the results published in Refs. [17,37] are compilations of data. In the second column, the characteristic $M\beta$ energies taken from Bearden [16] are also shown. It can be seen that, according to several authors [8–12,37], $E_{M_5} > E_{\mathrm{M}\beta}$ for Re, Os, Ir, and Pt, which is consistent with the test displayed in Fig. 4; whereas the E_{M_5} values taken from Refs. [7] and [17] are lower than the corresponding $M\beta$

TABLE I. Energy of the M_5 edge and the $M\beta$ line, in keV. When available, the estimated uncertainties in the last digits are indicated as numbers in parentheses. Underlined values correspond to the case $E_{M_5} > E_{M\beta}$. Values in brackets are tentative M_5 edge energies, arbitrarily chosen to be above the $M\beta$ line, as used in the assessments shown in Fig. 4.

	$E_{M\beta}$	E_{M_5}							
Z	Ref. [16]	Ref. [7,17]	This work	Ref. [37]	Ref. [8]	Ref. [9]	Ref. [10]	Ref. [11]	Ref. [12]
70	1.5675(4)	1.5278(4)		1.5187					
71	1.6312(4)	1.5885(4)							
72	1.6976(2)	1.6617(4)							
73	1.7655(3)	1.7351(3)		1.759				1.771(2)	
74	1.8349(3)	1.8092(3)		1.846	1.8483				
75	1.9061(3)	1.8829(3)	1.907(8)						
76	1.9783(3)	1.9601(3)	[1.99]	1.998		2.0017			
77	2.0535(3)	2.0404(3)	[2.06]	2.076		2.07993			
78	2.1273(4)	2.1216(3)[a]	[2.16]	2.153		2.16152	2.1710(3)		
79	2.2046(4)	2.2057(3)		2.241			2.2518(3)		
80	2.2825(4)	2.2949(3)		2.321					
81	2.3621(5)	2.3893(3)		2.409					
82	2.4427(5)	2.4840(3)							
83	2.5255(5)	2.5796(3)							2.603(2)

[a]Taken from Ref. [7]; 2.1211 keV according to Ref. [17].

characteristic energies. In the last column, the E_{M_5} binding energy for Re determined along this work is also included, as well as the values chosen for Os, Ir, and Pt to perform the test shown in Fig. 4.

V. CONCLUSION

The energy of the M_5 edge is critical when considering the self-absorption of $M\beta$ photons for certain elements of the sixth period. In opposition to the established E_{M_5} values, the present study suggests that these energies should be above the $M\beta$ emission energy for Re, Os, Ir, and Pt. Summarizing, the following can be stated:

(1) $E_{M\beta} > E_{M_5}$ for $70 \leqslant Z \leqslant 74$, in agreement with Refs. [7,17].

(2) $E_{M\beta} < E_{M_5}$ for $75 \leqslant Z \leqslant 78$, unlike Refs. [7,17] (in agreement with Refs. [9,10,37]).

(3) $E_{M\beta} < E_{M_5}$ for $79 \leqslant Z \leqslant 83$, in agreement with Refs. [7,10,12,17,37].

Consistently with the present remarks, the wavelength dispersive spectroscopy analysis performed for rhenium does not show a defined jump at the energy reported in Refs. [7,17]. In addition, the theoretical calculations of configuration energies and photoionization cross sections for rhenium led to an E_{M_5} value slightly above the $M\beta$ emission energy, which supports the conclusions stated above.

Surprisingly, the measurement of the binding energies studied here has not been faced by means of modern equipments, such as synchrotron experiments with high-resolution analyzing crystals. This evinces the importance of the present work carried out with commercial equipments using electron beams, and also invites researchers to find accurate values with sophisticated equipments, when available.

ACKNOWLEDGMENTS

This work was financially supported by the Secretaría de Ciencia y Técnica of the Universidad Nacional de Córdoba (Grant No. 32720200400177CB), Argentina, and also through the PICT2016-0285 and PICT2020-SERIE A-01931 grants from ANPCyT-FONCyT, Argentina, and the PIP11220200102421CO grant from CONICET, Argentina. The authors are also grateful to the Laboratorio de Microscopía y Análisis por Rayos X (LAMARX-UNC) and the Laboratorio de Microscopía Electrónica y Microanálisis (LABMEM-UNSL) where the experimental determinations were performed.

[1] P. Wu, Y. Yu, C. E. McGhee, L. H. Tan, and Y. Lu, Adv. Mater. **26**, 7849 (2014).

[2] F.-X. Ouf, P. Parent, C. Laffon, I. Marhaba, D. Ferry, B. Marcillaud, E. Antonsson, S. Benkoula, X.-J. Liu, C. Nicolas, E. Robert, M. Patanen, F.-A. Barreda, O. Sublemontier, A. Coppalle, J. Yon, F. Miserque, T. Mostefaoui, T. Z. Regier, J.-B. A. Mitchell, and C. Miron, Sci. Rep. **6**, 36495 (2016).

[3] Y. Ménesguen, M.-C. Lépy, Y. Ito, M. Yamashita, S. Fukushima, M. Polasik, K. Słabkowska, Ł. Syrocki, E. Węder, P. Indelicato, J. Marques, J. Sampaio, M. Guerra, F. Parente, and J. Santos, J. Quant. Spectrosc. Radiat. Transfer **236**, 106585 (2019).

[4] G. Greczynski and L. Hultman, Prog. Mater. Sci. **107**, 100591 (2020).

[5] V. Mackert, T. Winter, S. Jackson, R. Kalia, A. Levish, S. Lukic, J. Geiss, and M. Winterer, J. Phys. Chem. C **127**, 17389 (2023).

[6] A. B. Shick, E. Belsch, and A. I. Lichtenstein, Phys. Rev. B **108**, L180408 (2023).

[7] J. A. Bearden and A. F. Burr, Rev. Mod. Phys. **39**, 125 (1967).
[8] R. V. Zumstein, in *Proceedings of the Iowa Academy of Science* (Iowa Academy of Science, Inc., Des Moines, 1924), Vol. 31, pp. 384–385.
[9] R. A. Rogers, Phys. Rev. **30**, 747 (1927).
[10] A. J. M. Johnson, Phys. Rev. **34**, 1106 (1929).
[11] C. A. Whitmer, Phys. Rev. **38**, 1164 (1931).
[12] W. D. Phelps, Phys. Rev. **46**, 357 (1934).
[13] B. D. Shrivastava, J. Phys.: Conf. Ser. **365**, 012002 (2012).
[14] F. A. Stevie and C. L. Donley, J. Vac. Sci. Technol. A **38**, 063204 (2020).
[15] P. S. Bagus, E. S. Ilton, and C. J. Nelin, Surf. Sci. Rep. **68**, 273 (2013).
[16] J. A. Bearden, Rev. Mod. Phys. **39**, 78 (1967).
[17] F. Larkins, At. Data Nucl. Data Tables **20**, 311 (1977).
[18] A. Thompson, I. Lindau, D. Attwood, Y. Liu, E. Gullikson, P. Pianetta, M. Howells, A. Robinson, K.-J. Kim, J. Scofield, J. Kirz, J. Underwood, J. Kortright, G. Williams, and H. Winick, *Center for X-ray Optics Advanced Light Source, X-ray Data Booklet*, LBNL/pub-490, 3rd ed., edited by University of California (Lawrence Berkeley National Laboratory, Berkeley USA, 2009).
[19] A. Aguilar, G. Castellano, S. Segui, J. Trincavelli, and A. Carreras, J. Anal. At. Spectrom. **38**, 751 (2023).
[20] A. Bar-Shalom, M. Klapisch, and J. Oreg, J. Quant. Spectrosc. Radiat. Transfer **71**, 169 (2001).
[21] R. Bonetto, G. Castellano, and J. Trincavelli, X-Ray Spectrom. **30**, 313 (2001).
[22] C. T. Chantler, J. Phys. Chem. Ref. Data **29**, 597 (2000).
[23] S. Reed, Br. J. Appl. Phys. **16**, 913 (1965).
[24] M. Gryzinski, Phys. Rev. **138**, 336 (1965).
[25] C. S. Campos, M. A. Z. Vasconcellos, J. C. Trincavelli, and S. Segui, J. Phys. B: At., Mol. Opt. Phys. **40**, 3835 (2007).
[26] X. Llovet, C. Merlet, J. M. Fernández-Varea, and F. Salvat, Microchim. Acta **132**, 163 (2000).
[27] D. Bote, F. Salvat, A. Jablonski, and C. Powell, At. Data Nucl. Data Tables **95**, 871 (2009).
[28] J. Oreg, W. H. Goldstein, M. Klapisch, and A. Bar-Shalom, Phys. Rev. A **44**, 1750 (1991).
[29] M. Klapisch, J. L. Schwob, B. S. Fraenkel, and J. Oreg, J. Opt. Soc. Am. **67**, 148 (1977).
[30] C. C. Montanari, C. D. Archubi, D. M. Mitnik, and J. E. Miraglia, Phys. Rev. A **79**, 032903 (2009).
[31] A. Mendez, C. Montanari, and D. Mitnik, Nucl. Instrum. Methods Phys. Res., Sect. B **460**, 114 (2019).
[32] A. M. Mendez, D. M. Mitnik, and C. C. Montanari, in *Jack Sabin, Scientist and Friend*, Advances in Quantum Chemistry, edited by J. Oddershede and E. J. Brändas (Academic Press, Cambridge, MA, 2022), Vol. 85 pp. 157–175.
[33] N. R. Badnell, J. Phys. B: At. Mol. Phys. **19**, 3827 (1986).
[34] N. R. Badnell and M. S. Pindzola, Phys. Rev. A **39**, 1685 (1989).
[35] N. R. Badnell, J. Phys. B: At., Mol. Opt. Phys. **30**, 1 (1997).
[36] R. D. Cowan and D. C. Griffin, J. Opt. Soc. Am. **66**, 1010 (1976).
[37] Y. Cauchois and C. Sénémaud, *Wavelengths of X-Ray Emission Lines and Absorption Edges* (Pergamon Press, Pergamon, New York, 1978), Vol. 18.